

CYCLIC LOAD TESTING OF THREE HAUNCHED REINFORCED CONCRETE BEAM-COLUMN ASSEMBLIES

S.J. Thurston*

SYNOPSIS:

The paper describes the testing of three reinforced concrete haunched beam-column assemblies under incremented-static cyclic loading. The half or full size test units were based upon typical interior joints of external frames of multi-storey buildings designed to the current NZ loading code¹.

Hinge formation occurred in the beams and stable hysteretic behaviour was obtained up to model displacement ductilities of 6 (worst unit) to 18 (best unit). Corresponding prototype building ductilities are shown to be slightly higher. Tests results indicated the importance of matching the yield moment strengths in the haunch with the combined seismic and gravity load distribution.

1. INTRODUCTION:

Under severe seismic loading of structures with conventional beams, plastic hinging tends to concentrate at the beam ends with opposite sense on either side of the column. A wide vertical crack usually forms early at the beam-column interface. At relatively low building ductility factors, (DFs), the high section curvatures and consequent high flexural compressive strains required near the beam ends encourage concrete spalling and buckling of the compressive steel. Consequently heavy stirrups are required in this zone. Because yield of the flexural steel can penetrate well into the beam-column joint, the bar length over which the steel stresses change from yield tension to yield compression may be small and bond slip may occur. These problems are largely circumvented with carefully designed beam haunches. If the yield moment strength within the beam haunch closely follows the combined seismic plus gravity flexural loading demand, then at high loads a large spread of plasticity will occur. Thus relatively small maximum section curvatures will allow large beam rotations to develop without excessive cracking or concrete spalling.

To ensure a large spread of plasticity in seismic dominated frames it is recommended that the steel at the small end of the haunch be designed to yield first, with at least 5% strain hardening strength increase required here before the beam at the large end of the haunch yields. This will also ensure that high yield strains do not occur near the beam-column junction, with consequent yield penetration in the joint and a wide crack at the junction.

Haunch beam design has two further advantages which may or may not be offset by increased construction cost:

- (a) The vertical component of the force in the sloping portion of the haunch balances a significant portion of the applied shear, and thus less vertical beam reinforcing is required.

Under downwards shear this force is provided by bottom tension reinforcement and under upwards shear the thrust is developed by concrete compression. Further, because the haunch spreads the zone of plastic hinging, crack widths are smaller at corresponding deflections and more shear load can be carried by the concrete. However additional confining reinforcement is required to contain the bursting stresses developed at the bend in the bottom longitudinal reinforcement. The final version of the concrete design code⁹ allows haunch concrete close to the column to carry significant shear stress, being the sum of allowable concrete shear away from a plastic hinge zone plus a component proportional to the slope of the haunch.

- (b) Beam haunching leaves more room for building services to pass under the beam at locations away from the haunches which may allow a reduction in storey height.

2. LOAD APPLICATION:

Testing was performed on the MWD Structure Laboratory's strong-floor. The loading on units 1 and 3 adequately simulated seismic dominated loading on the assembly with points of contraflexure approximately at mid-height on the column and midspan of the beams as shown in Figure 1. Load was applied to the beam ends by independent hydraulic jacking systems providing downwards load (negative moment at the column face) through a strain-gauged tension yoke and upwards load through a compression load cell and rocker - roller system. A constant axial column load of approximately 0.65 f'c A_g was continuously checked and adjusted as necessary.

Unit 2 was tested as a simply supported beam (Fig. 1). Although this setup accurately simulates the moments in each half of the beam under seismic attack it does not test anchorage of the reinforcing steel in the joint, the shear strength of the joint, or check that the flexural strength of the column exceeds that of the beam. However as the joint and columns were capacity designed to be stronger than the beams framing into them the deficiencies of

*Design Engineer, Ministry of Works and Development, Wellington, N.Z.

the loading method were not considered significant.

More detail on the test setups can be found in references 3, 5 and 6 for units 1, 2 and 3 respectively.

3. DESCRIPTION OF TEST UNITS³:

In all test units (Fig. 3 - 5) transverse beam steel was placed in the joint to simulate the practical difficulties of reinforcement cage construction and placement of concrete in the congested joint region. Additional stirrups were placed at the ends of the haunch to carry the bursting forces caused by the bend in the bottom longitudinal beam steel. The columns and joints in Units 1 and 3 were capacity designed to be stronger than the beams for seismic loading causing yielding in either (but not both) planes of beams.

UNIT 1

The full size test unit model is a typical interior beam-column joint designed for the four storey Standard Minitch Teaching Block Structure. The ratio of the moment strengths at the large and small ends of the haunch is 1.15 but the gradient of moment applied during testing was 1.29, and thus yielding is expected to occur first at the beam-column interface. Problems were encountered when placing the concrete, and grouting was subsequently required near the bottom steel in the joint which probably reduced steel bond strengths. Since these tests the NZ Design Code, DZ 3101⁴ has limited the diameter of Grade 275 beam steel passing through interior joints to 1/25 of the column depth. That is 28 mm in this case rather than the 32 mm used. This code requirement is intended to prevent concrete-reinforcing bond failure during seismic load reversals although this should be less critical if plastic hinging occurs away from the joint.

UNIT 2

The full size test beam models typical second floor interior beams and column stub of the William Clayton four-storey, two-way frame building. The stirrups were used on the East beam and the gap (if any) between the longitudinal steel and stirrups shimmed with steel bolt nuts as necessary to ensure a reasonable positive direct bearing between stirrups and main bars. The average gap on the West beam of 6 mm was left open. However visual and recorded experimental results did not indicate a better performance of the East beam, thus indicating that a tight fit of stirrups may not be essential.

UNIT 3

The half scale test unit models typical transverse interior first floor beam and column of the National Library building. The test model includes the first filled in waffle slabs as shown in Fig. 5 as per the prototype. Details of test setup which are similar to those used for Unit 1 are shown in Fig 2.

4. INSTRUMENTATION:

Beam end deflections were measured to an accuracy of 0.1 mm by optically sighting through a surveyor's level onto scales attached to the beam. Beam rotations were measured over successive gauge lengths by 50 x 0.01 mm dial gauges attached between frames connected to the beam (Fig 6). Demountable mechanical strain gauges with 250 mm gauge lengths were used to measure surface strains along the joint panel diagonals. Electrical resistance strain gauges were used extensively to measure strains of beam and column flexural reinforcement, of column ties and joint stirrups both within and outside the joint. Recorded steel strains were reduced to stresses using a Bauehinger analysis computer program based on Ramberg-Osgood type equations.

5. RESULTS:

UNIT 1

Full details of test results on Unit 1 are described in Ref. 3. In summary, at cycles up to and including model deflection ductility factors of 6, (DF=6), (Fig 6) five major and a grid of minor cracks had formed along the haunch although they tended to be wider near the column and a crack of 5 mm at the beam-column junction was more than twice the width of other beam cracks. At DF=8 (Fig. 7) the concrete cover was lost on the underside of the beam haunches and during the second cycle the bottom longitudinal beam bars were slipping through the joint allowing cracks at the beam-column junctions to open in excess of 40 mm. This was attributed mainly to poor joint concrete although the shallowness of this particular haunch may have been contributed to yield penetration of the joint and consequent higher bond stresses.

A plot of moment at the column face versus deflection at the pull down point is plotted in Fig. 12. Reasonably satisfactory behaviour is demonstrated by the hysteresis loops with no significant loss of stiffness or load capacity through to the end of the DF=6 cycles. The degradation in the moment capacity following the first DF=8 cycle is mainly a result of the slipping of the bottom beam bars through the joint with some influence from the beam shear cracks.

The measured beam rotations within 330 mm of the column face were only marginally larger than those 330-660 mm from the column face up to the end of DF=6. The rotations between 660-990 mm from the column were about half those above at corresponding stages. (Note - the haunch length = 915 mm as shown in Fig. 3). Thus despite the loading moment gradient being greater than the beam moment strength gradient in the haunch as discussed in Section 4, a wide plastic hinge zone still developed in the haunch. However during the DF 8 cycles most of the increase in rotations occurred in the beam close to the column due to slipping of the bottom beam bars through the joint.

Longitudinal beam steel stresses through the joint region of the haunched unit are shown in Fig. 13 for the peak loading of the third cycle at 3/4 yield and at the

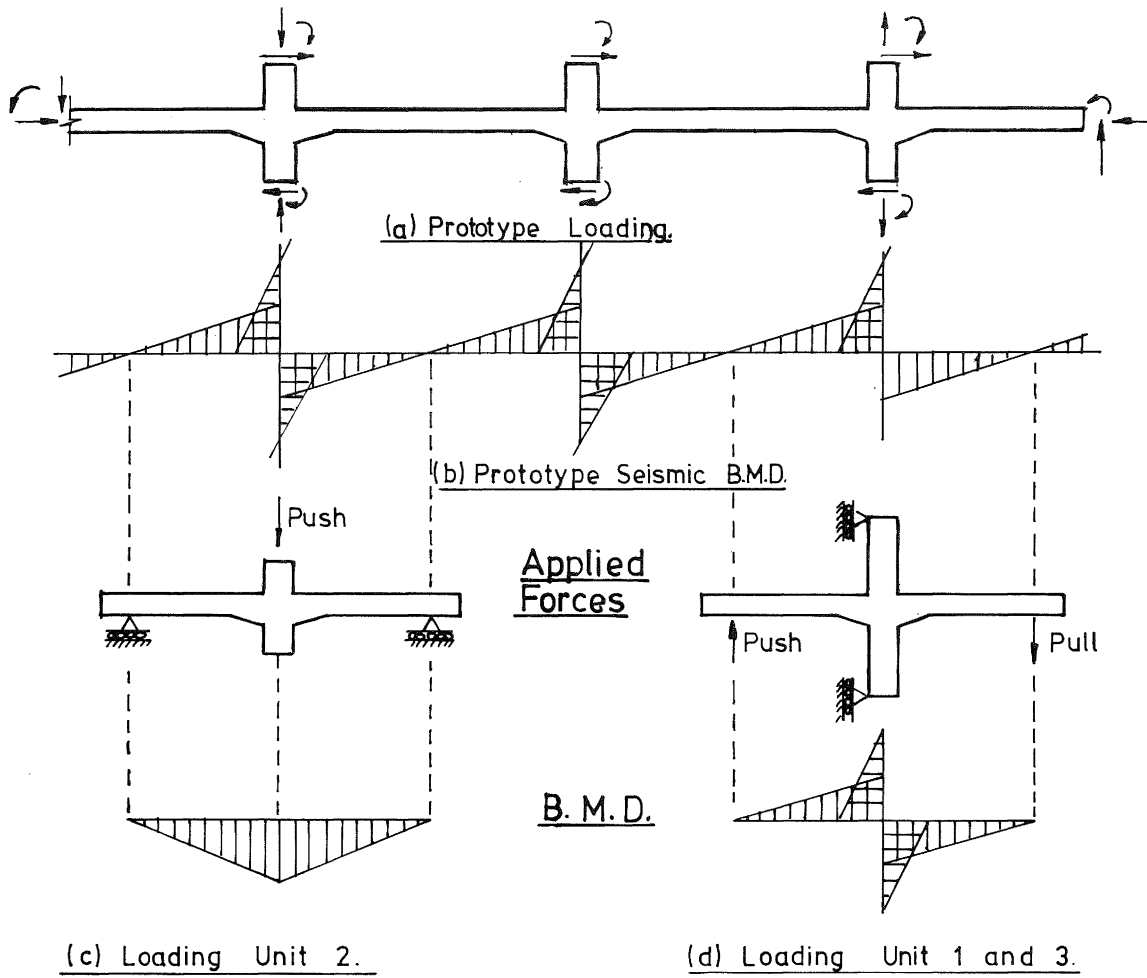


FIG. 1 - LOADING ON PROTOTYPE AND TEST UNITS

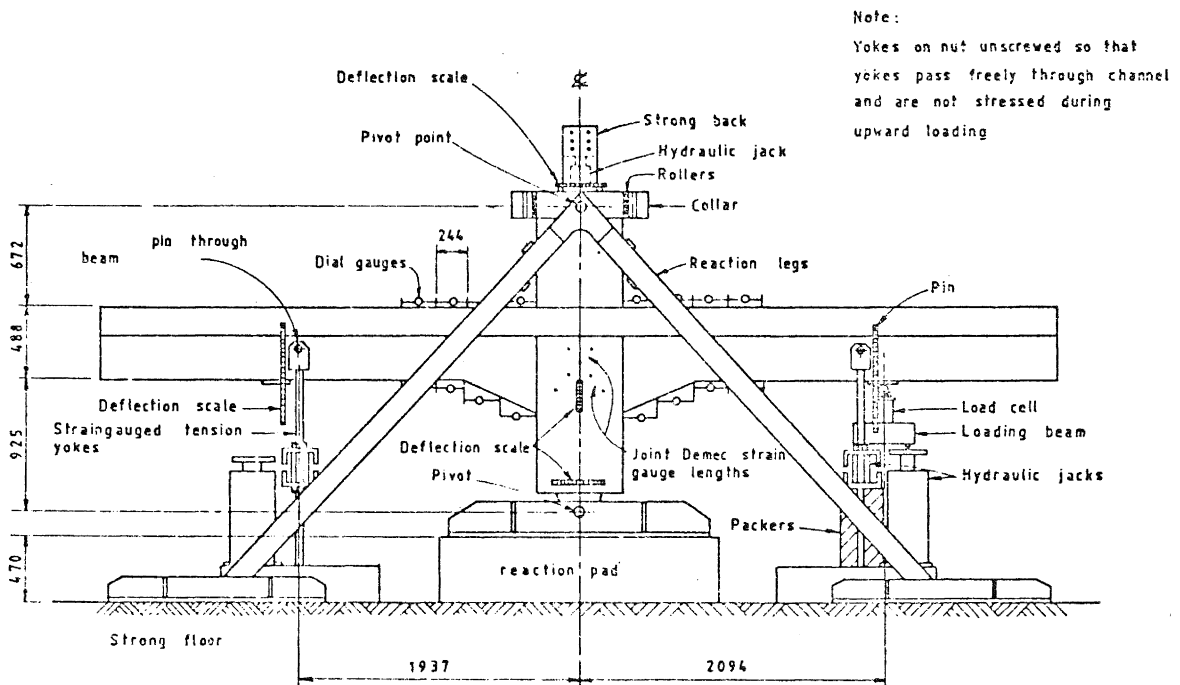


FIG. 2 - TEST SET-UP UNIT 3

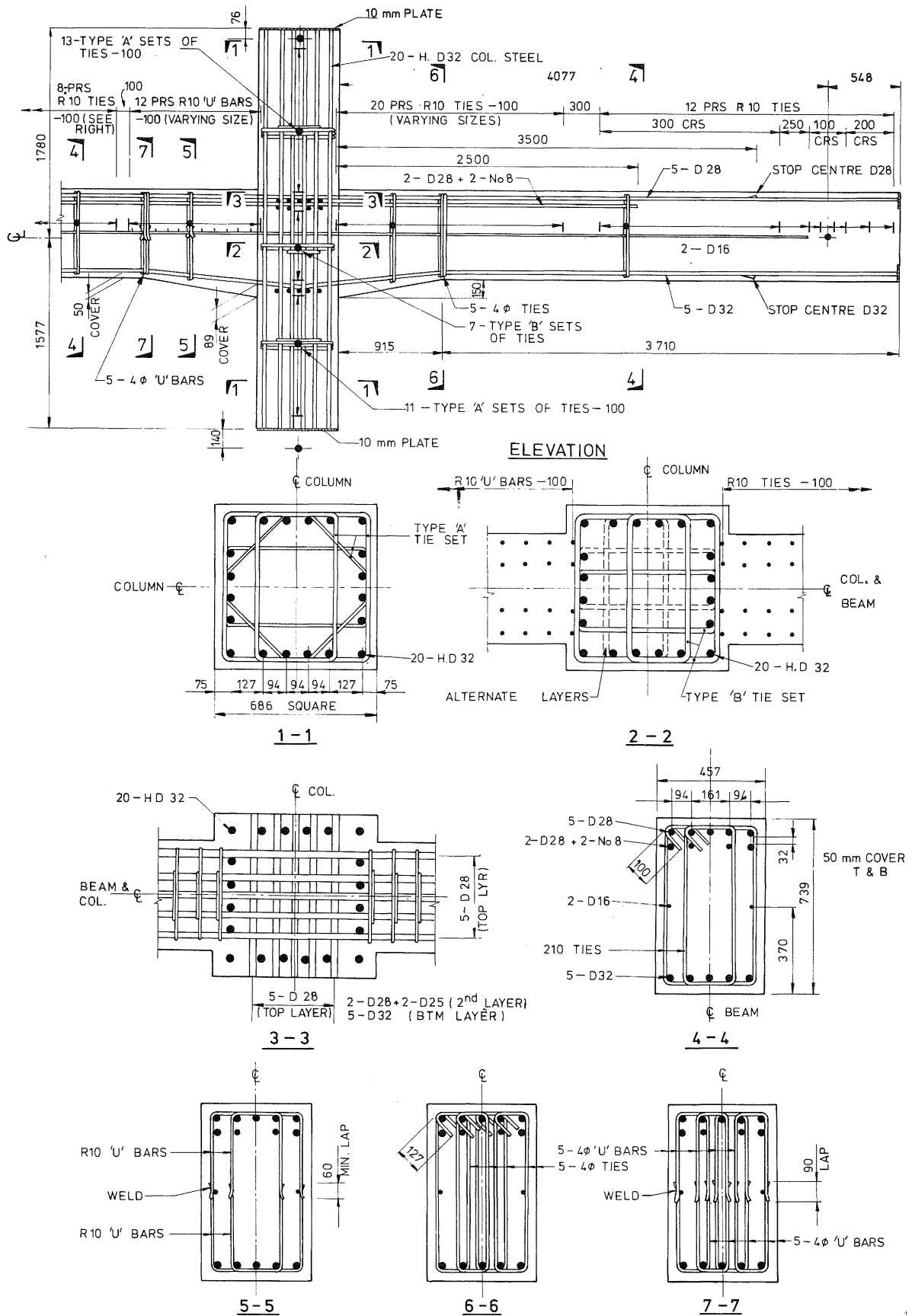


FIG. 3 - REINFORCING DETAILS - UNIT 1

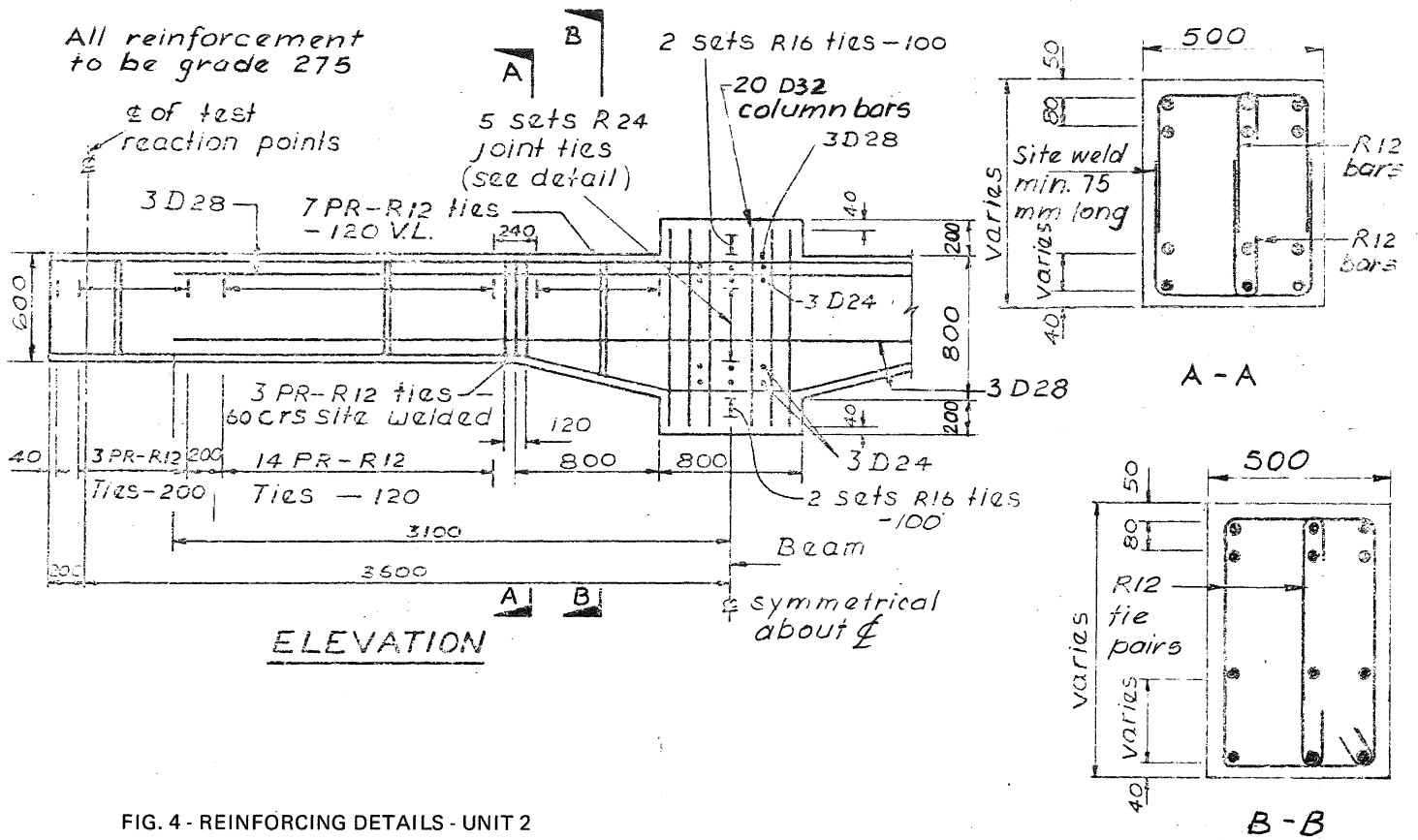


FIG. 4 - REINFORCING DETAILS - UNIT 2

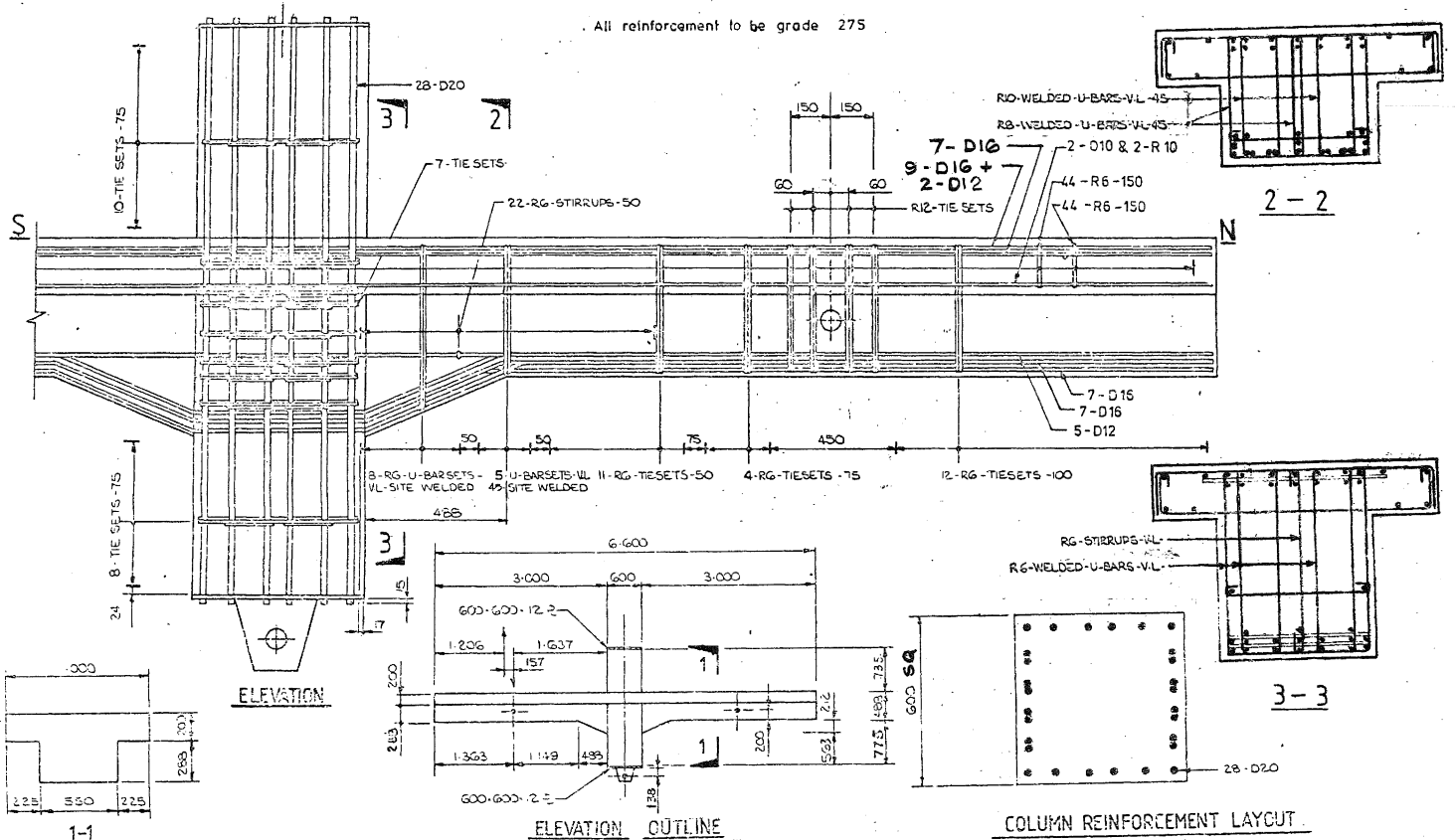


FIG. 5 - REINFORCING DETAILS - UNIT 3

first cycle for DF 2, 4 and 6. Compression yielding of the beam longitudinal reinforcement did not occur until the DF = 6 cycles. Tension yielding occurred for almost the entire haunch length from DF = 2 onwards.

Yield was reached in the longitudinal legs of some joint ties at DF=4 and in some legs of the majority of ties at DF=8. Thus although the actual horizontal shear reinforcement was less³ than 67% of DZ 3101⁴ and 85% of ACI⁷ recommendations the performance of the joint panel was satisfactory throughout the testing. Few recorded beam tie stresses in the haunch and at the bend in the longitudinal reinforcing reached yield stress.

UNIT 2

At the completion of two 3/4 yield cycles fine vertical cracks at centres of approximately one third beam depth had developed in the haunch region over the full beam depth. There was however no cracking at the beam-column junction at this stage. During the subsequent increased deformation cycles between DF=2 to DF=4 the number of cracks and crack propagation gradually increased until a network of cracks had developed. Apart from a little fretting at the edges of the cracks no spalling occurred until at DF=18 small areas (about 100 x 50) of cover concrete fell off (Fig.8). The very high ductility of the beam at this loading is evident in Fig. 9. The increase in the number of relatively fine cracks prevented excessive crack widths from being generated up to DF=12, and it was at subsequent greater deformations that crack widths started increasing significantly. (Fig. 14). The cracks widths at the beam-column junctions were relatively small.

The major cracks shown in Fig. 8 can be seen to be close to vertical indicating flexural rather than shear loading. As at peak loads the vertical component of thrust in the sloping portion of the haunch can be calculated to be more than half the applied shear loading, the absence of inclined cracking is not surprising.

A plot of applied load versus beam midspan deflection and the measured beam rotation at three pertinent zones along the beam are presented in Figs. 15 and 16 respectively. Although very large ductilities (over 18) were imposed on the beam there was little visual or measured deterioration. The "fatness" of the hysteresis loops, the absence of "pinching" effects, the small load reduction on repetitive cycles and the continuing increase in load at each new imposed deflection indicate excellent energy absorbing capacity and little degradation of the beam.

The peak stresses recorded in the stirrups increased with each successive larger ductility factor, but as even at DF=18 no recorded stress in the haunch stirrups exceeded half yield stress, lighter stirrups may have successfully been used. Note that the stirrups were designed according to DZ 3101⁴ which did not allow

advantage to be taken of the greater shear resistance of haunched beams. A small percentage of stirrups at the small end of the haunch, designed to contain bursting stresses at the bend in the longitudinal reinforcing, did reach yield stress at DF=8 and higher ductilities.

Peak measured longitudinal beam steel tensile stresses at DF=0.75 were close to 75% yield and at the predicted locations³, which provides confidence in the analysis and measurements. At peak loads at subsequent larger ductilities all the tensile steel and most of the compression steel in the haunch region was yielding.

UNIT 3

As with Unit 2, the two cycles to 0.75 yield load induced but a few vertical full depth cracks. However, there was minor cracking at the beam-column junction and diagonal cracking in the joint region. The number of cracks increased considerably during the cycles at DF=2 especially at the notch at the small end of the haunch. Crack widths were generally less than 0.5 mm. At DF=4 additional cracking further concentrated at the notches with crack widths reaching 3 mm being measured (see Fig. 10). At the South notch, where the bottom longitudinal bars were not crossed, (Fig 3), a wedge of concrete for the full width of the underside of the beam became loose, probably due to the bursting forces at the bend in the bottom bars. To prevent this the prototype design was modified by having a 800 radius rather than a sharp bend in the bars and by putting transverse steel between the bottom layers of steel to ensure adequate bearing of the upper bottom steel layer.

At DF=6 the plastic hinges lengthened to occupy all the haunch region and a distance of about beam depth/2 outside the haunch, with a network of cracks being developed. Minor spalling occurred beneath the South beam notch which increased at the DF=8 cycle. Spalling at the North beam notch was still not significant.

At DF=10 large spalling occurred at both notches with buckling of the bottom reinforcing bars when in compression. At DF=12 and 16 buckling of the bottom bars and spalling occurred to a greater extent at the notches and although the beam was still resisting large forces it was looking very distressed at this location with the cover concrete having been lost for half the beam depth. Eventually three bottom bars broke due to the high buckling bending strains. Some spalling also occurred at the upper regions of the flange close to the notches. The condition of the unit and huge deformations imposed at test completion, (DF=16), are shown in Fig. 11.

Plots of load versus beam deflection (corrected for movement at the column top) are presented in Fig. 17. The "fatness" of the hysteresis loops and absence of "pinching" effects indicate excellent energy absorbing capacity of the beams. Except at the second cycle at DF=16 (where the bars broke) there is little reduction in load at corresponding deflections of previous cycles and the peak resisted load at each increased deflection continues to increase. There is but small evidence of the buckling of the bottom bars in the curves.

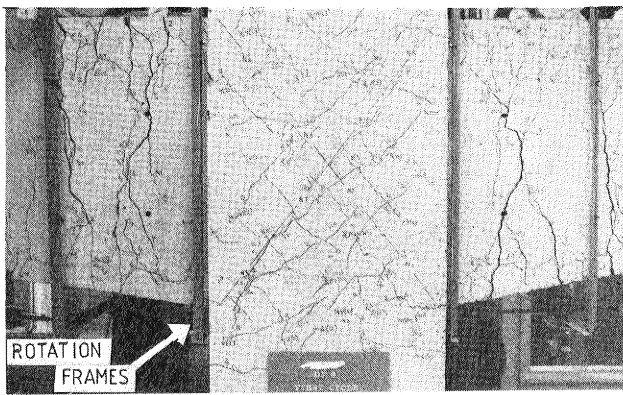


FIG. 6 - UNIT 1 AT D.F. = 6

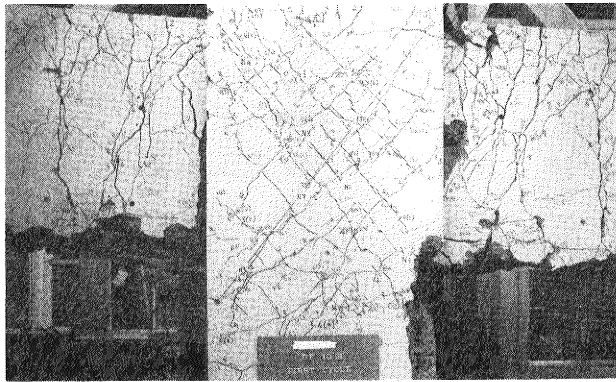


FIG. 7 - UNIT 1 AT D.F. = 10

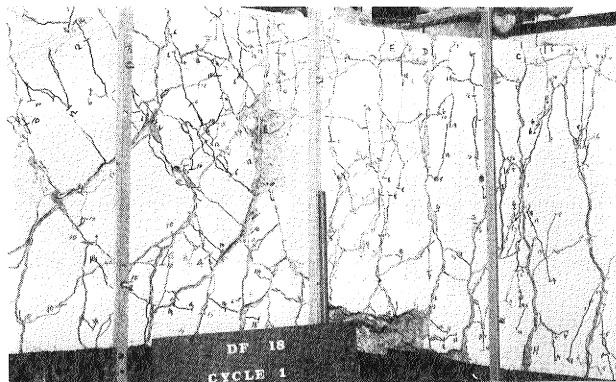


FIG. 8 - UNIT 2 AT D.F. = 18

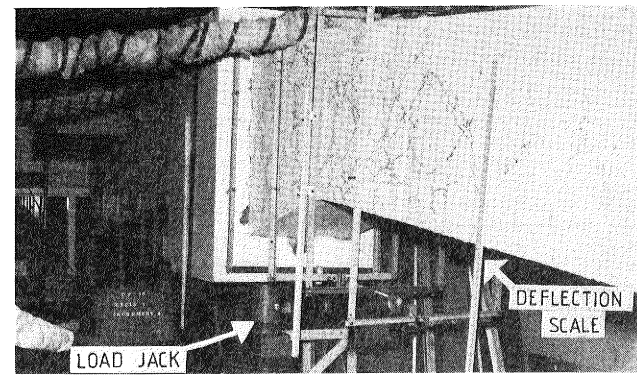


FIG. 9 - UNIT 2 AT MAXIMUM DEFORMATION

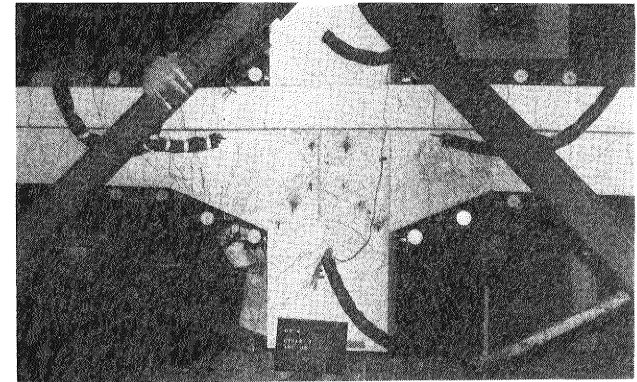


FIG. 10 - UNIT 3 AT D.F. = 4

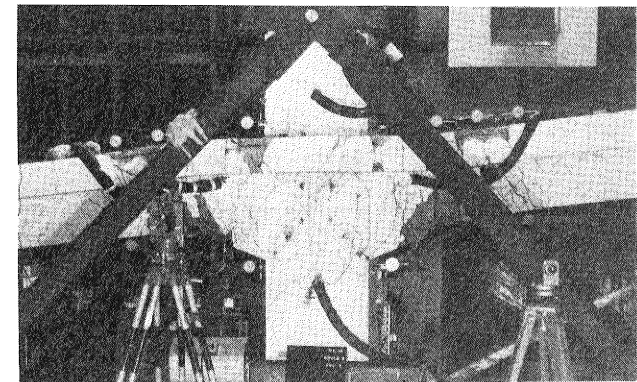


FIG. 11 - UNIT 3 AT MAXIMUM DEFORMATION

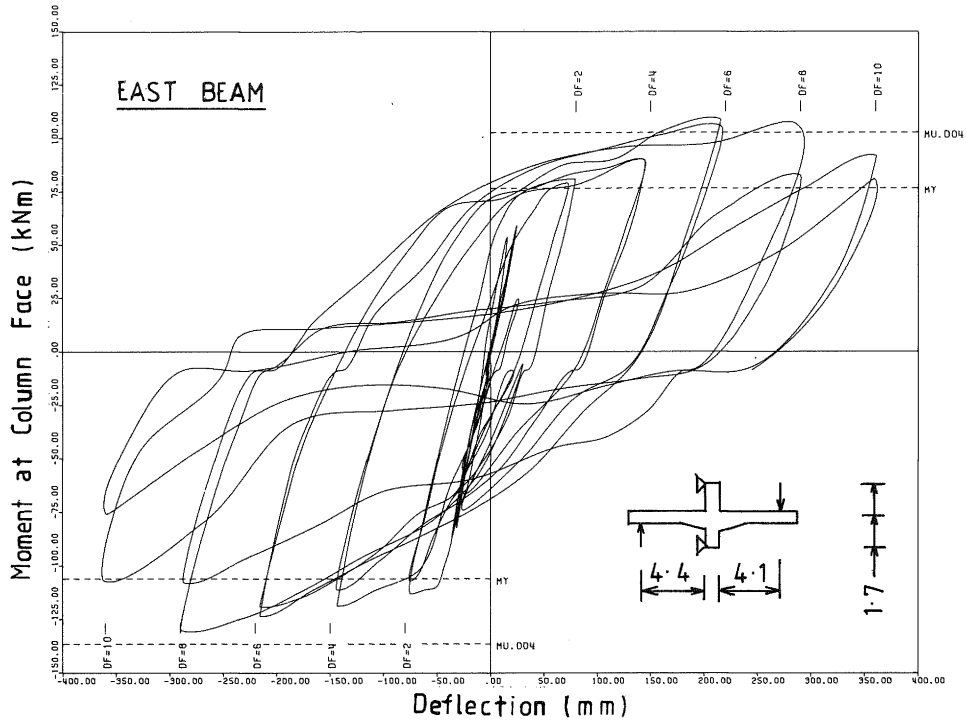


FIG. 12 - UNIT 1 - MOMENT DEFLECTION BEHAVIOUR

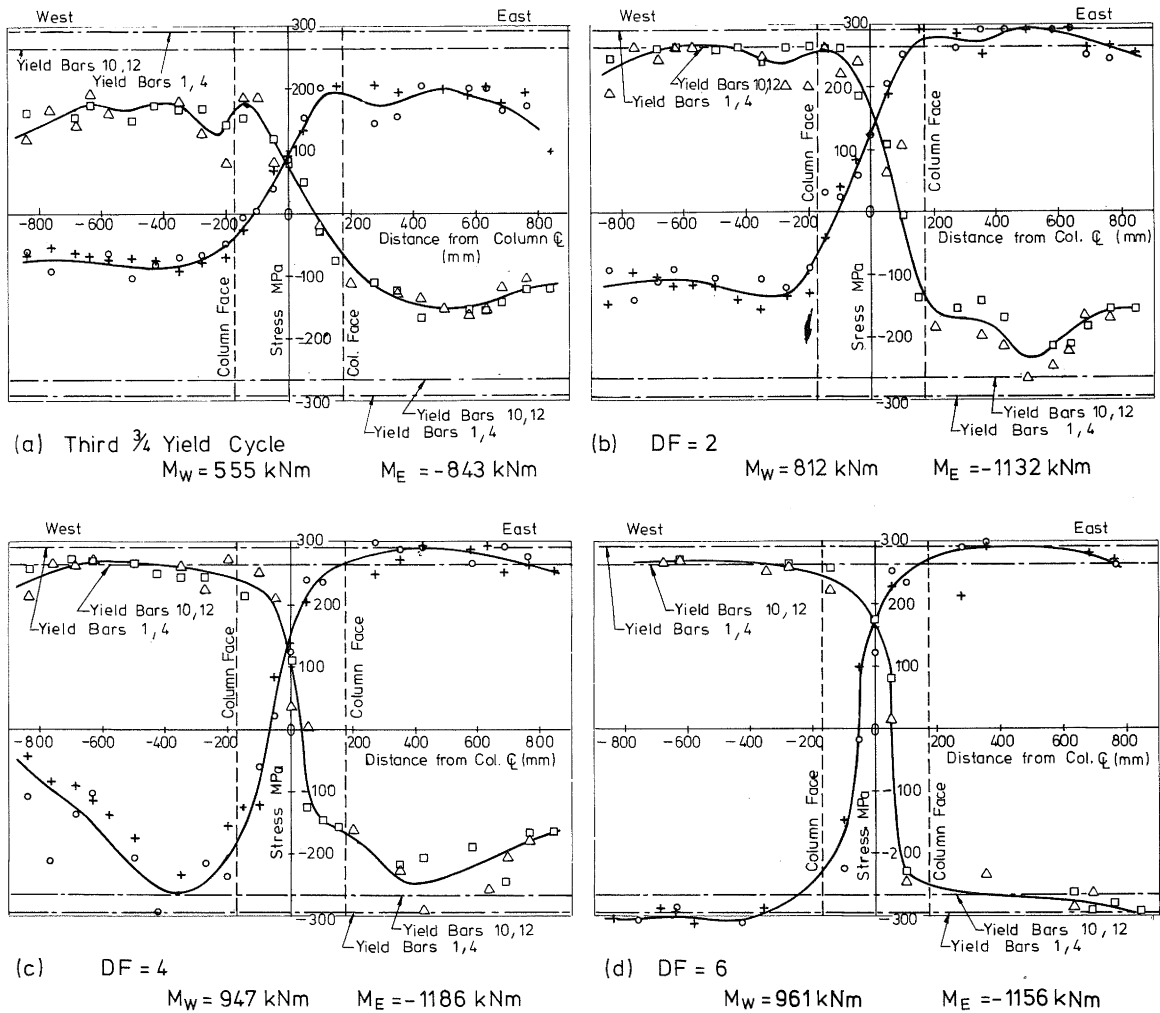


FIG. 13 - UNIT 1 - BEAM STRESS DISTRIBUTION

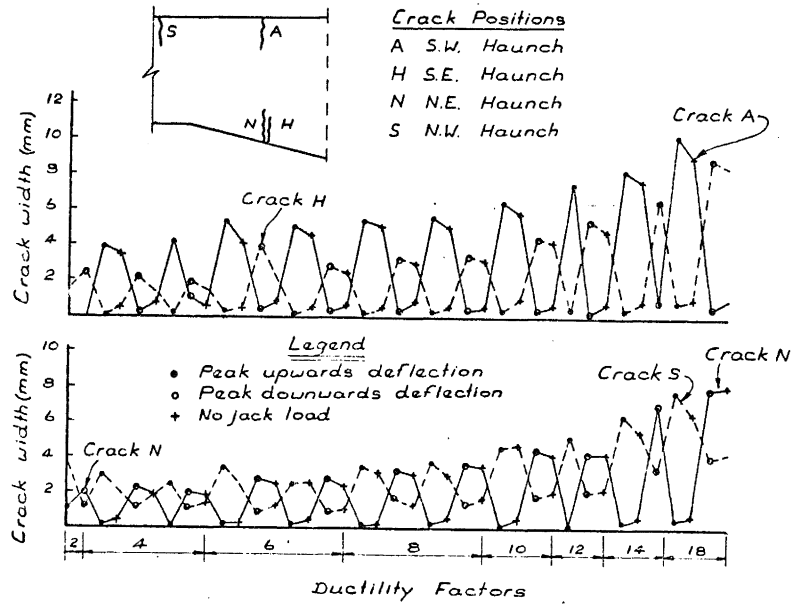


FIG. 14 - UNIT 2 - MEASURED CRACK WIDTHS

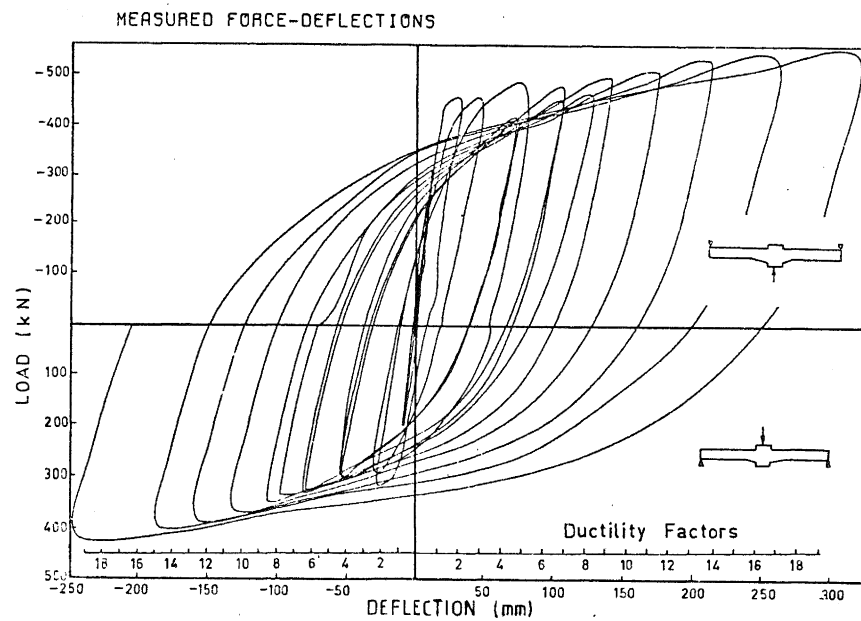


FIG. 15 - UNIT 2 - FORCE DEFLECTION BEHAVIOUR

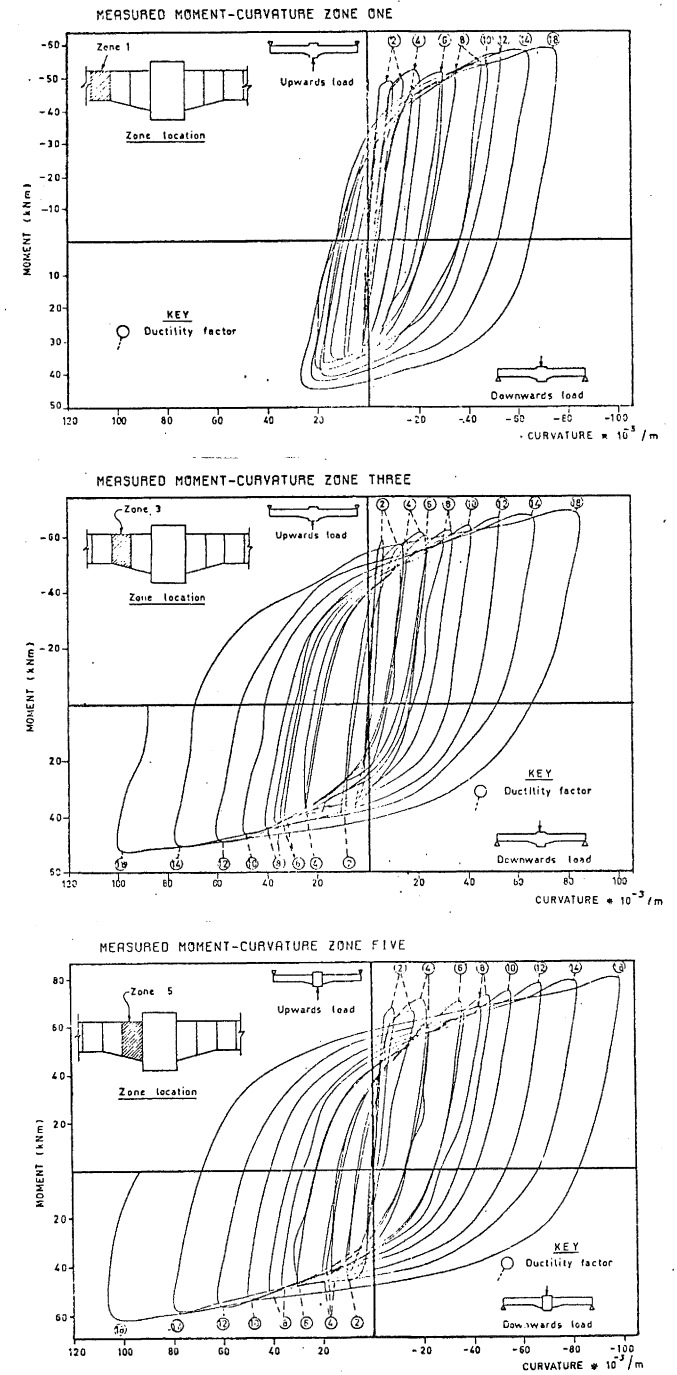


FIG. 16 - UNIT 2 - MOMENT CURVATURE RELATIONSHIPS

The measured moment-curvature relationship for zones in and close to the South haunch is presented in Fig. 18. Most of the rotation occurred in zone 3 (just inside the haunch) which approximately equals the sum of the rotations in zone 2 and 4. Thus a wide spread of plastic hinging occurred with the major plastic rotations occurring in the haunch just inside the notch.

Measurements of joint strains indicated that during the initial cycle when significant joint cracking occurs, the joint shear accounts for approximately 11% of total beam displacements, which reduces to about 5% from DF=6 onwards.

Some beam stirrups yielded at the small end of the South haunch at DF=2 but away from the notch the peak stresses in the stirrups quickly dropped to low values (less than 100 MPa). At higher ductility factors the zone of the yielding near the notch became larger, but even at DF=10 no stirrups in the haunch further away than 200 mm from the notch had reached stresses greater than 200 MPa. Stresses in stirrups in the North beam were significantly less than in the South beam because of the different steel layout.

Yielding of one joint tie occurred at DF=2 with yielding at a further tie at DF=4, but most ties remained elastic up to DF=6. From DF=8 onwards progressively more ties yielded. The results indicate that the joint had not been over-designed for shear. The measured peak longitudinal column bar stresses were close to, but did not exceed yield stress.

A good agreement was obtained between predicted and measured longitudinal beam steel stresses at DF=0.75. From DF=2 onwards all tension steel yielded over the full length of the haunch. However extensive yielding of the compressive steel did not occur until DF=6.

6. RELATIONSHIP BETWEEN BUILDING AND TEST UNIT DUCTILITY FACTORS:

Consider the deformation of a building subsequent to the formation of a "plastic" mechanism as shown in Fig. 19. Assuming that all plastic hinging develops simultaneously and at the onset of plasticity roof deflection is Δy , then from geometry and using the nomenclature of Fig. 19

$$(\Delta u - \Delta y) = r H \theta = r H \frac{\Delta_b}{L/2} \quad \dots (1)$$

Hence the building ductility factor μ_p is given by:

$$\mu_p = \frac{\Delta_u}{\Delta_y} = 1 + \frac{2rH\Delta_b}{L\Delta_y} \quad \dots (2)$$

The model ductility factor μ_m is given by $1 + \frac{\Delta_b}{\delta_y}$

where δ_y = test beam yield deflection

$$\text{Hence } \mu_p = 1 + \frac{2rH}{L} (\mu_m - 1) \frac{\delta_y}{\Delta_y} \quad \dots (3)$$

Park⁸ approximated Δ_y by:

$$\Delta_y = \frac{H^2}{6} (\phi_{c1} (r + 1/3) + \phi_{c2} + \phi_{c3} + \dots + \phi_{cr})$$

where ϕ_{ci} is the curvature in the column at the bottom of the i th storey at first beam yield. From Fig. 20, $\delta_y = 0.105\psi L^2$ for a typical haunched beam. If the following approximations are made the building and test unit ductility factors can be related as shown in Table 1, which predicts the building ductility factors to be larger than the model ductility factors.

$$(1) \quad \phi_{c1} = \phi_{c2} = \phi_{c3} = \dots = \phi_{cr}$$

- (2) If the building design was based on the strong column weak beam philosophy and if axial column load is small then ψ approximately = $2\phi_c$ (i.e. say column depth is $1/3$ greater than beam depth and at first yield in beam column steel has a peak stress of $2/3$ yield).

In real buildings, as all plastic hinges do not reach first yield together, the term 'building ductility' requires defining not only to clarify the type of ductility being expressed (i.e. displacement or rotational) and whether it is in terms of building centre of gravity or the top of the main portion of the building, but also what is taken as the 'yield' point must be defined.

There are three common definitions of 'yield':

- 1 When a significant number of plastic hinges have formed in the main resisting elements. (Without defining significant).
- 2 When yield first occurs in the main structural element or the earthquake code¹ load E calculated on the assumption of elastic behaviour, whichever is greater.
- 3 The point of intersection of the two straight portions of the load-deflection curve for the building.

The last definition applied to the roof displacement for Unit 3 was used by McKay⁶ to give the comparison of model displacement ductility to building displacement ductility.

The building displacement under an increasing code proportioned lateral load was determined using STRUDL. As STRUDL is an elastic analysis program plastic hinges were modelled by inserting pins with equal and opposite yield moments applied each side as the yield capacity is exceeded for each load increment. This method neglects any increase in yield moment due to strain hardening and if any plastic hinges should lose capacity for any reason during increasing applied lateral load this method will give a false picture.

From the computer output two typical 1st floor beam displacements were used to relate to building displacements and hence compare ductilities.

For the National Library frames the code¹

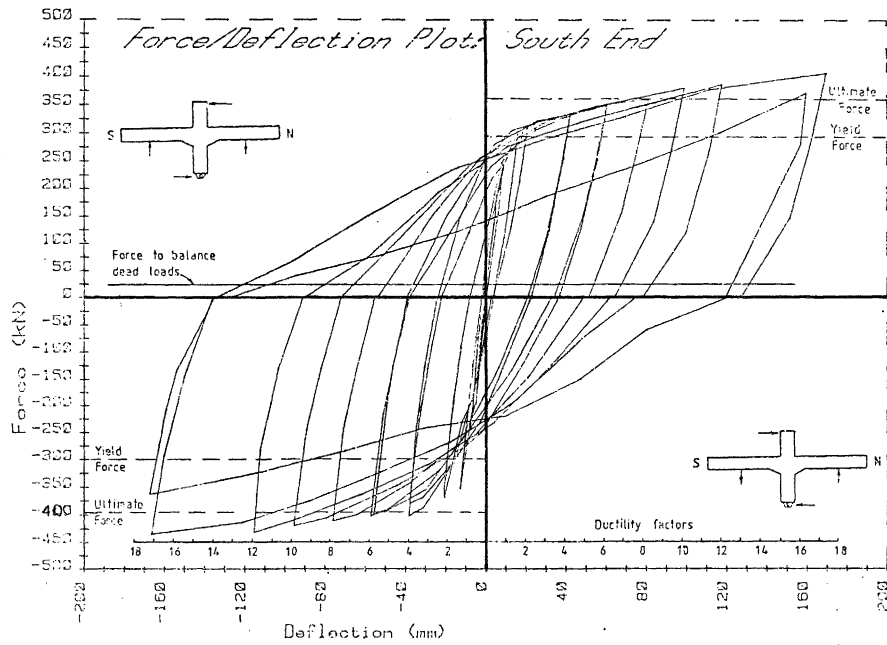


FIG. 17 - UNIT 3 - FORCE DEFLECTION BEHAVIOUR

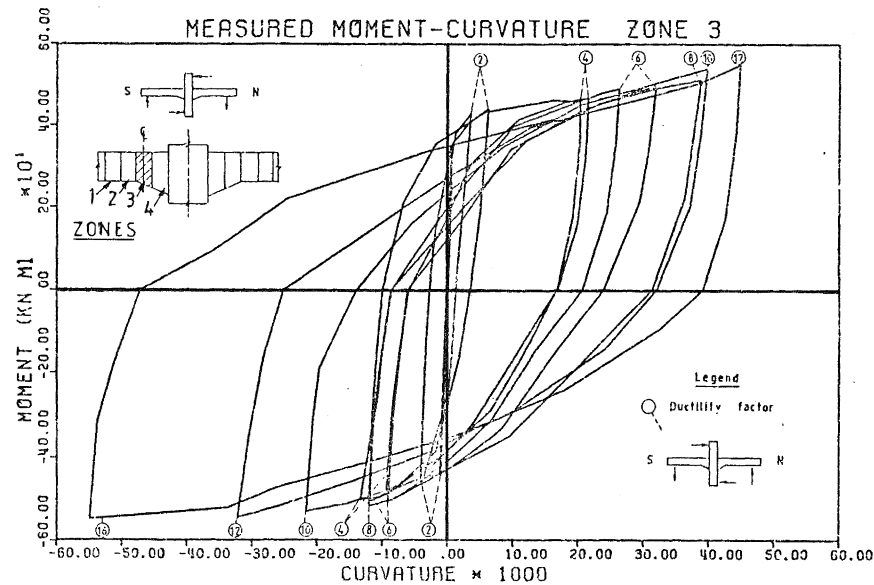


FIG. 18 - UNIT 3 - MOMENT CURVATURE RELATIONSHIP

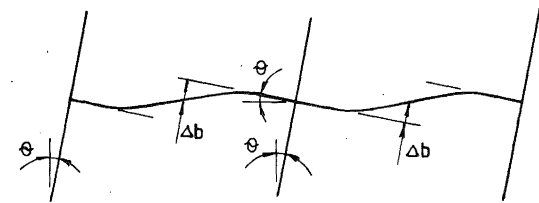
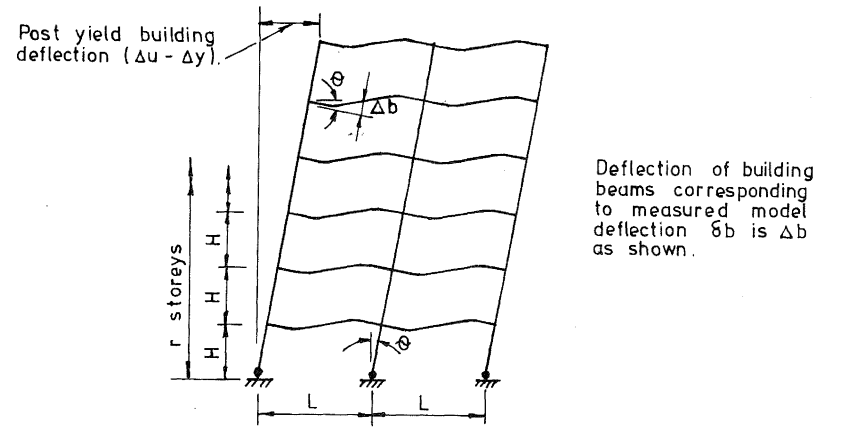
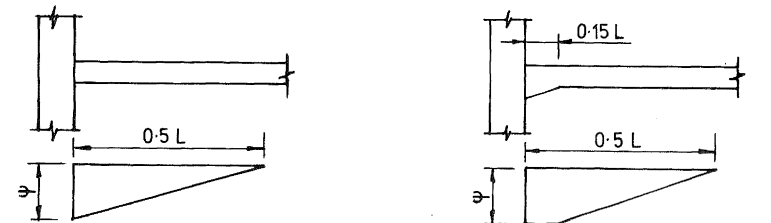


FIG. 19 - POST ELASTIC DEFORMATION OF BUILDING



Curvatures at first yield.

$$\delta_y = \psi \times \frac{(0.5L)^2}{3}$$

$$= 0.083 \psi L^2$$

$$\delta_y = \psi L^2 (0.15 \times 0.425 + \frac{(0.35)^2}{3})$$

$$= 0.105 \psi L^2$$

FIG. 20 - DEFLECTION OF TEST UNITS AT FIRST YIELD

TABLE 1 : CALCULATED PROTOTYPE
DUCTILITY FACTORS

Test Unit Ductility factor	L/H = 2		L/H = 1	
	r = 10	r = 4	r = 10	r = 4
1	1	1	1	1
2	3.6	3.7	2.3	2.4
4	8.8	9.2	4.9	5.1
8	17.3	20.2	10.1	10.6
16	40.0	42.2	20.6	21.6

TABLE 2 : COMPARISON OF BUILDING AND TEST UNIT
DUCTILITY FACTORS AS COMPUTED FROM
STRUCL ANALYSIS

<u>TEST UNIT 3 DUCTILITY</u>	<u>PROTOTYPE BUILDING DUCTILITY</u> (L/H=2)
1	0.98
2	2.03
4	4.39
6	6.86

seismic design coefficient is 0.135g, with first yield of a single plastic hinge forming at 0.192g. The frame yield was assumed at 0.211g with 71% of available hinges formed and peak plastic load was 0.229g.

Computed STRUDL results in Table 2 indicate that the building ductilities are in close agreement with beam deflection ductilities which were defined as model ductility factors for the test units. On the other hand Table 1 predicts approximately twice the building ductility for a corresponding model ductility and $L/H=2$. The difference is attributed to be mainly due to the error in the assumption that all plastic hinges occur simultaneously. In any event it is clear that model ductility factors will be at least as great as overall building ductility factors for most buildings.

7. CONCLUSIONS:

Deformation hysteresis loops obtained during incremental-static cycling of Units 2 and 3 were "fat" and stable and exhibited no "pinching" up to ductility factors of > 18 and $12 - 16$ respectively. Plastic hinging was spread uniformly throughout the haunch with Unit 2 but tended to concentrate at the small end of the haunch in Unit 3. Attracting the hinges away from the joint protected the joint in each case. Relatively small cracks were distributed throughout the haunch. An excessively wide crack was not developed at the beam-column junction as occurs when the beam is not haunched.

The ductilities obtained for these haunched beam units can be compared with those measured for conventional beams by both Beckingsale¹⁰ and Blakeley et al¹¹ for full size units where intermediate column bars were used and column width/bar diameter = 24. Beckingsale¹⁰ found pinching of the hysteresis loops and bar slip at $DF=6$ although high axial column load improved this performance. However the hysteresis loops in Blakeley et al¹¹ tests did not degenerate until $DF=10$.

Fat stable loops were developed in Unit 1 only up to $DF=6$. This was attributed to the seismic loading gradient being greater than the haunch over-strength moment gradient, and to poor joint concrete. This combination led to bond failure in the beam reinforcement through the joint.

The vertical component of the thrust in the sloping portion of the haunch helps resist shear, and the volume of shear reinforcement can be correspondingly reduced.

Carefully proportioned beam haunches enhance the aseismic structure resistance, and if building services can be placed to utilise the lesser beam depth near midspan haunching may well be an economic proposition.

REFERENCES:

1. New Zealand Standard for General Structural Design and Design Loadings for Buildings, NZS 4203 : 1976 Part 3, "Earthquake Provisions" Standards Association of New Zealand, Wellington, 1976.
2. Park, R. and Paulay, T. "Reinforced Concrete Structures" John Wiley and Sons 1974.
3. Blakeley, R.W.G., Edmonds, F.D., Megget, L.M. and Wood, L.H., "Cyclic Load Testing of Two Refined Reinforced Concrete Beam-Column Joints." Proc. of 2nd South Pacific Regional Conference on Earthquake Engineering, Volume 2, pp 459-492.
4. Draft New Zealand Code of Practice for the Design of Concrete Structures, DZ 3101, Standard Association of New Zealand, Wellington, 1978.
5. Thurston, S.J. "Testing of a Reinforced Concrete Haunched Beam Under Simulated Seismic Loading". Ministry of Works and Development, New Zealand, Central Laboratories Report No. 5-79/2.
6. Harichandran, R.S. "Cyclic Testing of a Reinforced Concrete Haunched Beam Column Joint". Ministry of Works and Development, New Zealand, Central Laboratories Report No. 5-80/6.
7. ACI-ASCE Committee 352, Recommendation for Design of Beam-Column Joints in Monolithic Reinforced Concrete Structures. ACI Journal, July 1976, pp 375-393.
8. Park, R. "Ductility of Reinforced Concrete Frames Under Seismic Loading." N.Z. Engineering, Volume 23, November 1968, pp. 427-435.
9. New Zealand Code of Practice for the Design of Concrete Structures, NZS3101, Standards Association of New Zealand, Wellington, 1982.
10. Beckingsale, C.W. "Post Elastic Behaviour of Reinforced Concrete Beam-Column Joints" Research Report 80-20 University of Canterbury, Department of Civil Engineering.
11. Blakeley, R.W.G., Megget, L.M. and Priestley, M.J.N., "Seismic Performance of Two Full Size Reinforced Concrete Beam-Column Joint Units", Bulletin of the New Zealand National Society for Earthquake Engineering, Vol. 8, No. 1, March 1975.